

Modeling the crop transpiration using an optimality-based approach

LEI HuiMin¹, YANG DaWen^{1†}, Stanislaus J. Schymanski² & Murugesu Sivapalan³

¹ State key Laboratory of Hydro-Science and Engineering, Tsinghua University, Beijing 100084, China;

² Max Planck Institute for Biogeochemistry, Postfach 10 01 64, 07701 Jena, Germany;

³ Departments of Geography and Civil and Environmental Engineering, University of Illinois at Urbana-Champaign, IL61801, USA

Evapotranspiration constitutes more than 80% of the long-term water balance in Northern China. In this area, crop transpiration due to large areas of agriculture and irrigation is responsible for the majority of evapotranspiration. A model for crop transpiration is therefore essential for estimating the agricultural water consumption and understanding its feedback to the environment. However, most existing hydrological models usually calculate transpiration by relying on parameter calibration against local observations, and do not take into account crop feedback to the ambient environment. This study presents an optimality-based ecohydrology model that couples an ecological hypothesis, the photosynthetic process, stomatal movement, water balance, root water uptake and crop senescence, with the aim of predicting crop characteristics, CO₂ assimilation and water balance based only on given meteorological data. Field experiments were conducted in the Weishan Irrigation District of Northern China to evaluate performance of the model. Agreement between simulation and measurement was achieved for CO₂ assimilation, evapotranspiration and soil moisture content. The vegetation optimality was proven valid for crops and the model was applicable for both C₃ and C₄ plants. Due to the simple scheme of the optimality-based approach as well as its capability for modeling dynamic interactions between crops and the water cycle without prior vegetation information, this methodology is potentially useful to couple with the distributed hydrological model for application at the watershed scale.

crop transpiration, CO₂ assimilation, optimality, feedback, ecohydrological model

1 Introduction

Northern China is one of the most important grain-producing regions in the country. However,

Received November 25, 2008; accepted December 1, 2008

doi: 10.1007/s11431-008-6008-z

†Corresponding author (email: yangdw@tsinghua.edu.cn)

Supported by the National Natural Science Foundation of China (Grant No. 50679029), the National Basic Research Program of China (“973”) (Grant No. 2006CB403405), and the Foundation of State Key Laboratory of Hydro-Science and Engineering of Tsinghua University (Grant No. sklhse-2006-A-02)

due to rapid economic development and population growth, this area is now undergoing a serious water crisis. For example, per capita renewable water is less than half of the water scarcity threshold in three Northern China rivers, the Yellow River, the Huaihe River, and the Haihe River, at 520, 470 and 530 m³, respectively^[1].

Runoff, a function of the dry climate and uneven temporal rainfall distribution, is the main cause for water stress in Northern China. Taking the Yellow River basin (the drainage area is 753000 km²) as an example, the mean annual precipitation is only 570 mm, whereas the mean annual runoff is 58 billion m³, with about 60% concentrated in the wet season. A further cause of water stress results from the ever-increasing and excessive water demand due to population growth, with concomitant demands for water for food production and industrial and municipal development^[1].

Agriculture is a particularly large water use in Northern China, constituting 84% of total water consumption in this region. Much of this is a reflection of poor water-use efficiency in irrigation practices, which has led to serious environmental problems in this region, such as river dry-up and groundwater overdrafts^[2]. Water conservation, based on improving the water use efficiency in agriculture, is recognized as a feasible and promising way to solve this problem. Therefore, it is necessary to be able to quantify the actual crop water consumption (i.e. transpiration), and also to understand the interaction between the atmosphere, water and a crop. Modeling crop transpiration is therefore a fundamental problem in hydrology that has proven to have significant difficulties. Current hydrological models, in general, primarily focus on the dynamic processes of runoff generation and flow routing, while evapotranspiration is usually modeled using a simple parameterization scheme. In current hydrological models, the most common approach for modeling crop transpiration uses the crop coefficient method based on the Penman-Monteith equation^[3]. Land surface models^[4] use an electrical analog form to describe water fluxes, then employ a complex parameterization of canopy resistances. However, the vegetation parameters used in these methods need to be calibrated based on the local observations, which is problematic when a model is employed for prediction under the climate change. In addition, although most current SVAT (soil-vegetation-atmosphere transfer) models have already simulated the biophysical interactions between the vegetation and the atmosphere, dynamic changes of vegetation have not been incorporated into these models^[5,6]. Therefore, the two-way feedback between vegetation and the atmosphere and water has not been modeled appropriately.

Vegetation optimality is based on natural evolution theory and considers that vegetation is in an optimality status via its long-term adaptation to the ambient environment. This approach does not need any calibration of vegetation parameters by using local data, but aims at predicting correlations^[7]. Although there have been a few applications of the vegetation optimality approach in hydrology^[7-9], these were all tested in natural ecosystems. Vegetation optimality in agricultural land is still unstudied.

Agricultural land differs from a natural ecosystem because of the strong impacts of human activities, such as irrigation, fertilization, harvesting, and weeding. For better management of water resources, the dynamic feedback between crops and water balance, and consequently crop water consumption under different management conditions, such as irrigation in the agricultural land, needs to be understood. Based on a previous optimality-based ecohydrological model, the present study aims to validate the optimality hypothesis for crops, and to study model performance on the simulated crop properties, including transpiration, CO₂ fluxes and water balance in an agricul-

tural ecosystem, based on long-term continuous field measurements.

2 Model description

A coupled vegetation optimality model^[10] that has been applied successfully in a native savanna ecosystem near Darwin, Australia was used for the agricultural modeling. The canopy was represented by two “big leaves”. One big leaf with invariant size represented perennial vegetation while the big leaf with variable size represented seasonal vegetation (e.g. grasses). In the present study, it is assumed that crops are similar to the annual grasses, so that all processes associated with perennial trees were removed in the model used here.

The crop canopy was allowed to vary with its vegetation cover. The root system was expressed using two parameters of root depth and root surface area. Root depth was assumed to be invariant (at 1 m), while the root surface area was allowed to vary on a daily time scale. Thus, the model consists of above-ground and below-ground parts (Figure 1). The above-ground part is composed of a photosynthetic model and a stomatal conductance model, in which the canopy properties (vegetation cover and electron transport capacity) and stomatal conductance were modeled based on two optimality principles. The below-ground part is composed of a water balance model and a root water uptake model that contains the optimization of root surface area.

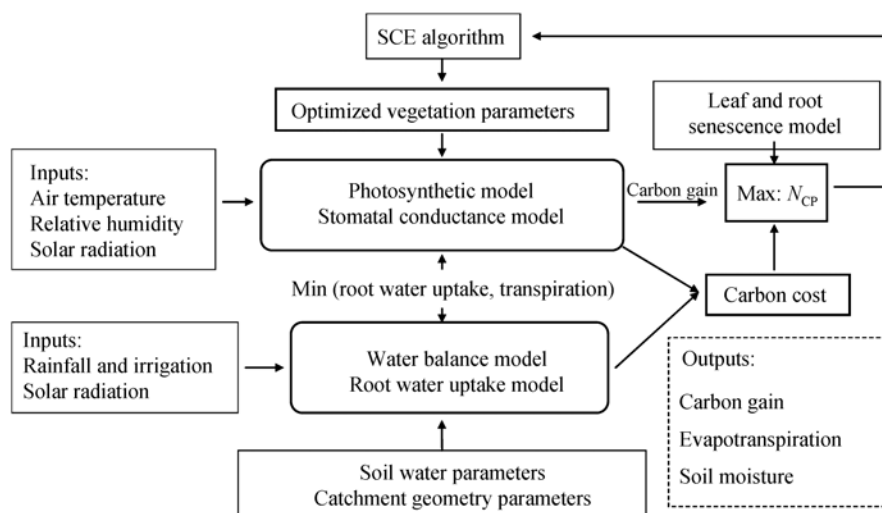


Figure 1 General diagram of the model.

2.1 Optimality principles and their formulations

2.1.1 Maximum N_{CP} hypothesis. The canopy properties were optimized using the maximum net carbon profit principle, which assumed that the “Net Carbon Profit” (N_{CP}) of the plant will be maximized if the plant has co-evolved with its environment over a long period of time. The Net Carbon Profit was defined as the difference between carbon gained by photosynthesis and carbon costs for maintenance of the organs involved in its uptake. The objective function of this optimality principle is given by ref. [10] as

$$N_{CP} = A_g - R_f - R_r - R_v, \quad (1)$$

where A_g denotes the net CO₂ assimilation, which is the benefit of N_{CP} , while the costs of N_{CP} are represented by leaf turnover cost (R_l), root maintenance cost (R_r) and water transport cost (R_v).

2.1.2 Carbon gain. The net CO₂ assimilation (A_g) is the difference between the carboxylation rate, A_c and leaf respiration, R_l . The carboxylation rate is estimated by a C₃ plant photosynthesis model^[11]. For simplicity, it is assumed that the photosynthetic rate is only limited by photosynthetic electron transport rate, J_A . The functional dependence of net CO₂ assimilation on electron transport rate (J_A), stomatal conductivity (G_s), the mole fraction of CO₂ in the air (C_a , 381 μmol/mol presently at this site), leaf respiration (R_l) and the CO₂ compensation point (Γ_*) has been formulated elsewhere^[7] and will only be summarized here:

$$A_g = \frac{1}{8}(4C_a G_s + 8\Gamma_* G_s + J_A - 4R_l) - \frac{1}{8}\sqrt{(-4C_a G_s + 8\Gamma_* G_s + J_A - 4R_l)^2 + 16G_s \Gamma_* (8C_a G_s + J_A + 8R_l)}. \quad (2)$$

The electron transport rate was calculated by ref. [10] as

$$J_A = J_{\max} \left(1 - e^{-\frac{\alpha I}{J_{\max}}} \right) M_A, \quad (3)$$

where J_{\max} is the electron transport capacity, I is solar radiation, α is a constant with the value of 0.3, and M_A is the vegetation cover of the crop. While leaf respiration was modeled as a linear function of the potentially maximal rate of A_g (A_{\max} , which is obtained by assuming light-saturation and infinite G_s)^[7]:

$$R_l = A_{\max} c_{Rl} = \frac{c_{Rl} J_{\max} (C_a - \Gamma_*)}{8(C_a + 2\Gamma_*)}, \quad (4)$$

where c_{Rl} is a constant parameter with a value of 0.07 (see Table 1). The dependence of J_{\max} on temperature and on its reference value at 25°C ($J_{\max 25}$) was parameterized following ref. [12]:

$$\frac{J_{\max}}{J_{\max 25}} = e^{\frac{\frac{H_a(T_a - 298)}{298 R_{\text{mol}} T_a} \left[\left(e^{\frac{H_d(T_{\text{opt}} - 298)}{298 R_{\text{mol}} T_{\text{opt}}} - 1 \right) H_a + H_d \right]}{\left(e^{\frac{H_d(T_a - T_{\text{opt}})}{R_{\text{mol}} T_a T_{\text{opt}}} - 1} \right) H_a - H_d}}, \quad (5)$$

where the molar gas constant (R_{mol}) was taken as 8.314 J · mol⁻¹ · K⁻¹, and H_a and H_d are the parameters (see Table 1). The temperature dependence of CO₂ compensation point, Γ_* for C₃ plants (winter wheat) was estimated using eq. (12) of ref. [12], in which the parameters were estimated from tobacco (*Nicotiana tabacum*, L. cv W38):

$$\Gamma_* = 0.00004275e^{\frac{126.946(T_a - 298)}{R_{\text{mol}} T_a}}, \quad (6)$$

where it is assumed that the air temperature represents leaf temperature.

The photosynthetic model for C₄ photosynthesis is quite different from that for C₃ plants^[13]. However, this can be described with the same equations at the canopy scale simply by employing different parameter values^[9]. Therefore, the C₃ photosynthetic model is also used for the C₄ maize

Table 1 Summary of the parameters of the model

Symbol	Description	Value/Unit	Source
α	Quantum yield of electron transport	0.3 mol/mol	Common value
c_{Rl}	Leaf respiration coefficient	0.07	ref. [14]
R_{mol}	Molar universal gas constant	$8.31 \text{ J} \cdot \text{mol}^{-1} \cdot \text{K}^{-1}$	Constant
H_a (wheat)	Rate of exponential increase of J_{max} with temperature	56.0 kJ/mol	ref. [15]
H_a (maize)		(average value)	ref. [16]
H_d (wheat)	Rate of decrease of J_{max} with temperature above T_{opt}	196.6 kJ/mol	ref. [15]
H_d (maize)		(average value)	ref. [16]
T_{opt} (wheat)	Optimum temperature for electron transport	25°C	ref. [17]
T_{opt} (maize)		35°C	ref. [18]
Γ^* (wheat)	CO ₂ compensation point in the absence of respiration	Eq. [12]	ref. [12]
Γ^* (maize)		$1.4 \times 10^{-6} \text{ mol/mol}$	ref. [19]
tcf (wheat)	Leaf turnover cost coefficient	2.38×10^{-7}	Personal communication with Jens Kattge
tcf (maize)		2.22×10^{-7}	
c_{Rr}	Root respiration rate per volume of fine roots	$0.0017 \text{ mol} \cdot \text{s}^{-1} \cdot \text{m}^{-3}$	ref. [20]
r_r	Mean radius of fine roots	$0.3 \times 10^{-3} \text{ m}$	ref. [21]
c_{rv}	Cost coefficient in eq. (9)	0.8×10^{-6}	Calibrated
a	Molecular diffusion coefficient of CO ₂ in air	1.6	ref. [22]
f	Evaporation factor	0.5	Calibrated
Ω_r	Root resistivity to water uptake per unit root surface area	1.019 s	ref. [20]
T_{base} (wheat)	Base temperature for growing degree day	0°C	ref. [23]
T_{base} (maize)		10°C	ref. [24]
S_l (wheat)	Threshold for leaf and root senescence	1729 degree days	ref. [24]
S_l (maize)		1445 degree days	ref. [25]
C_l (wheat)	Threshold of the cease of growing of root	1360 degree days	ref. [24]
C_l (maize)		1011 degree days	ref. [25, 26]
α_{vG}	The empirical parameters of the van Genuchten water retention model	2.0 m^{-1}	ref. [27]
n_{vG}		1.41	

crop in this study, on the premise that Γ^* was set at $1.4 \times 10^{-6} \text{ mol/mol}$, which is an average value for summer maize^[19].

2.1.3 Carbon cost. The leaf turnover cost was approximated as^[10]

$$R_f = 2.5 \times tcf \times M_A, \quad (7)$$

where tcf is 2.38×10^{-7} for winter wheat and 2.22×10^{-7} for maize (personal communication with Jens Kattge). These were both estimated from an average of the observed leaf mass per area of wheat and maize species. The root maintenance cost was modeled as a function of root radius (r_r) and root surface area (S_{Ar})^[20]:

$$R_r = c_{Rr} \left(\frac{r_r}{2} S_{Ar} \right), \quad (8)$$

where c_{Rr} is root respiration rate per volume of fine roots (Table 1). The water transport cost was formulated as

$$R_v = c_{rv} M_A y_r, \quad (9)$$

where c_{rv} is a calibrated value^[10]. In this study, it was set to be 0.8×10^{-6} , which led to realistic model results.

2.1.4 Stomatal conductance and transpiration rate. Crop transpiration was simply modeled as a diffusive process:

$$E_t = aG_s(W_l - W_a) = aG_sD_v, \quad (10)$$

where a is a constant which is set to be 1.6 following ref. [22]. W_l and W_a denote the mole fractions of water vapor inside and outside the leaf, respectively^[20]. It was assumed that the air inside the leaf was saturated. Stomatal movement was modeled by an optimality hypothesis^[22]. It is postulated that $A_g - \lambda E_t$ should be maximized with a constant value of λ during a period by adjusting leaf scale stomatal conductivity, G_s :

$$\frac{\partial E_t / \partial G_s}{\partial A_g / \partial G_s} = \frac{\partial E_t}{\partial A_g} = \lambda. \quad (11)$$

Combining eqs. (2), (10) and (11), crop transpiration can be finally derived as:

$$E_t = \frac{aD_v [C_a (J_A - 4R_l) - 4(J_A + 2R_l)\Gamma_*]}{4(C_a - 2\Gamma_*)^2} + \frac{\sqrt{3} \sqrt{aD_v J_A \Gamma_* (\lambda C_a - 2aD_v + 2\lambda\Gamma_*)^2 (\lambda C_a - aD_v + 2\lambda\Gamma_*) [C_a (J_A - 4R_l) - (J_A + 8R_l)\Gamma_*]}}{4(C_a + 2\Gamma_*)^2 (\lambda C_a - aD_v + 2\lambda\Gamma_*)}, \quad (12)$$

where λ is a constant within one day, and is parameterized as a function of the average matrix suction head of each soil layer (h_i) in the root zone^[10]:

$$\lambda = c_{\lambda f, s} \left(\sum_{i=1}^{i_{r,s}} h_i / i_{r,s} \right)^{c_{\lambda e, s}}, \quad (13)$$

where the parameters $c_{\lambda f, s}$ and $c_{\lambda e, s}$ are assumed to represent the long-term adaptation of the crop to its environment, and $i_{r,s}$ denotes the deepest soil layer accessed by roots. A high value of λ would mean that a large decrease in canopy transpiration would lead to only a small decrease in canopy CO₂ uptake. Thus, we would expect that so-called ‘water stressed’ vegetation would operate at a lower λ than vegetation with ample water supply.

2.2 Water balance and root water uptake

The water balance model is a spatially lumped model in which only the geometrical catchment and soil hydraulic properties should be changed according to the local conditions. The elementary watershed was divided into a saturated layer and an unsaturated layer whose thicknesses were variable. The unsaturated layer was then subdivided into several sub-layers whose thickness was set at 0.5 m. The water balance components include infiltration, water fluxes between soil layers, runoff, root water uptake, and soil evaporation processes, and their detailed formulations can be found elsewhere in ref. [20]. Here, only soil evaporation and root water uptake will be described.

2.2.1 Soil evaporation. Soil evaporation (from the unsaturated zone, E_{su} , and from the saturated zone, E_{ss}) was modeled as a linear function of surface soil water, global irradiance and irradiated soil surface fraction^[10]:

$$E_{su} = f \frac{I(1 - 0.8(1 - M_A))\omega_u S_{u,1}}{\lambda_E \rho}, \quad (14)$$

$$E_{ss} = f \frac{I(1 - 0.8(1 - M_A))\omega_o}{\lambda_E \rho}, \quad (15)$$

where λ_E is the latent heat of vaporization, 2.45×10^6 J/kg, and ρ denotes the density of water, 1000 kg/m^3 . 0.8 is an empirical value. An adjustment factor, $f (=0.5)$ was added to reflect the differences among soil types. ω_u and ω_o are the saturated and unsaturated surface area fractions, respectively, and $s_{u,l}$ is the average saturation degree of the top soil layer.

2.2.2 Root water uptake and root optimization. Root water uptake from each soil layer ($Q_{r,i}$) was modeled using an electrical circuit analogy^[20]:

$$Q_{r,i} = S_{Ar,i} \left(\frac{h_{r,i} - h_i}{\Omega_r + \Omega_{s,i}} \right), \quad (16)$$

where $h_{r,i}$ is the matric suction head in the roots, Ω_r is root resistivity to water uptake, and $\Omega_{s,i}$ is the resistivity to water flow towards the roots in the soil, which was formulated as a function of unsaturated hydraulic conductivity ($K_{\text{unsat},i}$), root radius and root surface area density in soil layer i ($S_{\text{Adr},i}$):

$$\Omega_{s,i} = \frac{1}{K_{\text{unsat},i}} \sqrt{\frac{\pi r_r}{2 S_{\text{Adr},i}}}. \quad (17)$$

The optimization problem for the root system is only the minimization of costs while meeting the water demand by the canopy^[20]. If root water uptake is less than the water demand by the canopy, the root surface area would increase, and would decrease if the root water uptake is more than the water demand.

2.3 Leaf and root senescence

In the original model^[10], the phenology was modeled as a result of the optimization of foliage cover in response to the seasonal light and water availability. However, the assumption of an optimal phenology is unrealistic for a crop ecosystem, where it is largely determined by the farmer's chosen crop cycle and the crops' senescence process. For example, winter wheat is sown in the autumn when the solar radiation has just started to reduce and the wheat senesces in the summer when radiation reaches its maximum. Therefore, crop senescence needs to be considered in the model.

Crop senescence is an age-dependent deterioration process at the cellular, tissue, organ, or organismal level, that leads to death or the end of the life span. The mechanism is very complicated and still unclear^[28]. A simple and empirical parameterization of leaf and root senescence was incorporated into the model to constrain the optimization. The growing degree day (GDD), usually used in agronomy to predict the development of crop^[29], is used in the model:

$$GDD = \sum (T_{\text{mean}} - T_{\text{base}}), \quad (18)$$

where the base temperature T_{base} is 0°C for wheat^[23] and 10°C for maize^[24]. T_{mean} is the daily mean air temperature. Two thresholds of growing degree days were set to control the development of crop, one for the leaf and root senescence (S_t), and the other for cessation of root growth (C_t).

In this region, summer maize needs an average value of 1445 degree days from sowing to maturity^[25], while winter wheat needs a typical value of 2200 degree days from sowing to maturity^[24]. As the leaves of maize are still alive when the grain is harvested, while the leaves of wheat are already dead, we assumed that wheat leaves started to senesce after the milking stage, but after the maturity stage for maize. Thus, S_t was set to be 1729 (the degree days needed from sowing to

milking) and 1445 degree days for wheat and maize, respectively.

In the original model, the roots were only optimized for the uptake of water. In reality, root growth depends both on the relationship between root water uptake and canopy water demand and also is closely related to carbon allocation^[30]. Root production usually increases for a given time, then remains relatively constant for a period, followed by a decline, even when the root water uptake is less than the water demand by the canopy^[31]. We assumed that roots stop growing at anthesis stage^[30], thus C_t was set to be 1360^[24] and 1011^[25,26] degree days for wheat and maize, respectively.

3 Study area and measurement

3.1 Study area

The study site (N36°39', E116°03') is located in the center of the Weishan Irrigation District (~450 km south of Beijing) along the downstream of the Yellow River in Northern China, with a total irrigated area of 3400 km². The climate is temperate and semi-humid, with about 581 mm mean annual precipitation and 1950 mm mean annual pan evaporation (Φ 20 cm). Approximately 70% of the annual precipitation is concentrated in the wet season (July to September), resulting in development of wheat in the dry season (March to June) depending on water diverted from the Yellow River (205 mm mean annual water during 1990–2007). The mean annual air temperature is 13.3°C. The domain vegetations are winter wheat and summer maize, which are rotated in cultivation. The growing season is from early October to mid-June for winter wheat and from mid-June to early October for summer maize.

The terrain, which is an alluvial land of the Yellow River, is very flat, about 24–40 m above the sea level with an average gradient of 1: 7500. The soil has thick silt-loam layer consisting of approximately 32% sand and 10% clay. The site is situated between two parallel rivers (about 7 km from both rivers). The riverbeds are very shallow because of silting sediments. In terms of catchment conceptualization^[20], this area was interpreted as having an average depth of the pedosphere of 3.0 m, and an average channel elevation of 2.0 m, from the reference datum. The empirical parameters of the van Genuchten water retention model were taken from the typical properties of silt loam^[27].

3.2 Measurement

A 10-m tall tower was erected to install flux and meteorological instruments above the crop canopy. Half-hourly fluxes of momentum, carbon dioxide, sensible heat (H) and latent heat (λE) were recorded using the eddy covariance system (CSAT3, Campbell Scientific, Inc.; LI7500, LI-COR, Inc.) at a height of 3.6 m. The flux data were recorded at 10 Hz. Meteorological data were recorded at 10-min intervals, including air temperature and humidity (HMP45C, Vaisala Inc.), downward and upward solar and long-wave radiation (CNR1, Campbell Inc.), downward and upward photosynthetically active radiation (PAR) (LI190SB, Licor Inc.), and precipitation (TE525, Campbell Inc.). Soil temperature and soil water content (two profiles) were measured at 5, 10, 20, 40, 80, 160 cm depths using temperature sensors (Campbell-107, Campbell Scientific Inc.) and time domain reflectometry (IT/MZ, TRIME Inc.); soil heat fluxes (G) were measured at 3 cm depth (HFP01SC, Huks Inc.). The groundwater table was measured in a well near the tower. Soil respiration was measured in the winter wheat season in 2006, at noon once every two weeks (LI820, Licor Inc.).

The measurement points were selected close to the tower so that surface soil temperature and soil water content could be obtained from the soil profiles.

The daily average PAR albedo, which was derived from the hourly upward and downward PAR measurements, was selected to represent the crop development. The PAR albedo is related to plant greenness and scales negatively with leaf area index, implying that it can capture the phenological events and canopy structure^[32]. The spikes in the flux data were removed^[33], then small gaps were filled using linear interpolation, while large gaps were filled using the gap-filling methodology presented by ref. [34]. The missing meteorological data were gap-filled by the space interpolation of nearby meteorological stations, using an angular distance weighting method^[2].

A number of unit conversions of the observed data were made to be compatible with the model^[7]. To obtain the estimated crop transpiration and CO₂ assimilation from the measured values, the observed canopy CO₂ exchange was partitioned into soil respiration (R_e) and net CO₂ assimilation (A_g), while the observed evapotranspiration of soil-crop system was partitioned into soil evaporation and crop transpiration. Soil respiration was estimated by a simple equation^[35]:

$$R_e = ae^{bT_s}, \quad (19)$$

where T_s is the soil surface temperature, a and b are parameters calibrated by the observed data. Soil evaporation was estimated by the soil surface moisture and soil surface temperature^[7]:

$$E_s = G_{\text{soil}} (W_s - W_a), \quad (20)$$

where W_s and W_a denote the mole fraction of water in the laminar layer immediately above the soil and the atmosphere, respectively. G_{soil} is a calibrated parameter. Unfortunately, the measured soil evaporation data from the study site are unavailable for calibration. As an alternative, this was set based on the measurements from a nearby site^[36].

4 Results and discussion

Hourly meteorological measurements (including precipitation, air temperature, air humidity and PAR) as well as the irrigation data (estimated from the soil moisture profile) from 2005-03-18 to 2007-10-17 and daily meteorological data (2004-10-01 to 2005-03-17) interpolated from nearby sites were used to drive the model. There were six crop seasons during this period, with the first season being a winter wheat season. Long-term adaptation of vegetation to the environment was modeled by the optimization of two parameters: $c_{\lambda f, s}$ and $c_{\lambda e, s}$. This optimization was performed using the Shuffled Complex Evolution algorithm^[37] which searches the parameter space for the global optimum by re-running the simulation. During each run, electron transport capacity ($J_{\text{max}25}$), vegetation cover (M_A) and the root surface area ($S_{Ar, i}$) were optimized dynamically on the daily scale. (The daily increment of vegetation cover was set at 0.02 for wheat, 0.05 for maize, and the daily increment of $J_{\text{max}25}$ was set at 1% of its actual value for wheat and 5% for maize). The parameters of winter wheat and summer maize were optimized independently for their corresponding growing seasons.

When the growing degree days reached the threshold for cessation of root growth, the optimization of root surface area stopped. Likewise, when it exceeded the thresholds of leaf and root senescence, the optimization of M_A , $J_{\text{max}25}$ and $S_{Ar, i}$ stopped and was replaced by a forced linear decline until the harvest day was reached. On the harvest day, M_A and the root surface area were set at 0.0, and $J_{\text{max}25}$ was set at a minimum value (50×10^{-6} mol/m²). Because the exact harvest day was

arbitrarily determined by farmers during the harvest period, it was set roughly to June 15 for the winter wheat and October 15 for the summer maize. For simplicity, the sowing day of the subsequent crop was assumed to be the same as the harvest day of the previous crop.

We aimed as far as possible to not require any information about the local vegetation or any parameters calibrated with observations. Thus, only two parameters c_{rv} (eq. (9)) and f (eqs. (14, 15)) were calibrated according to local measurements, while all others were obtained from literature surveys (Table 1), and are either average values or typical values.

4.1 Optimized canopy properties

The optimized vegetation cover had six cycles corresponding to the variations of observed PAR albedo (Figure 2). In the winter, winter wheat is in its dormant stage and the disagreement between optimized and observed values may imply that the mechanism of wheat dormancy is not captured by this model. The optimized J_{\max} ranged from 8 to 411 $\mu\text{mol}/\text{m}^2 \cdot \text{s}$ and it basically corresponded to the observed values for J_{\max} in the range between 17 and 372 $\mu\text{mol}/\text{m}^2 \cdot \text{s}$ ^[38]. The disagreement may be due to the lumped canopy conceptualization. The optimized root surface area ranged from 0.0 to 0.11 m^2 per unit ground area. However, it should be noted that the root surface area simulated was the minimum necessary to meet the canopy water demand^[20]. In reality, many more fine roots are needed to explore the nutrient pools in the soil; therefore, the optimized root surface area was much smaller than the observations (e.g. the live fine root area index is 79.1 for temperate grassland) given by ref. [39].

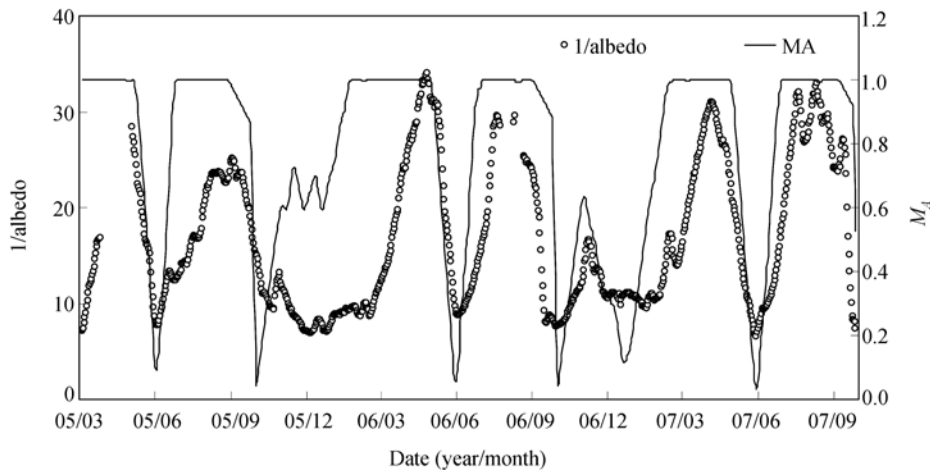


Figure 2 Weekly average of the optimized vegetation cover and observed 1/albedo.

The optimized $c_{\lambda f,s}$ and $c_{\lambda e,s}$ were 4.0×10^3 , -2.0 for wheat and 8.4×10^3 , -2.0 for maize, which means that the λ of maize was much higher than that of wheat, with the same matric head, and which suggests that maize was more wasteful of water. At the same time, the high values of λ of both wheat and maize mean that a very similar amount of CO_2 uptake could be achieved with significantly less water use, and imply that more water could be conserved.

4.2 Simulation of CO_2 assimilation, evapotranspiration and soil moisture content

Figures 3–5 show the comparisons of CO_2 assimilation, evapotranspiration and soil water saturation $((\theta - \theta_r)/(\theta_s - \theta_r))$, where θ , θ_r and θ_s are the actual, residual and saturated soil water content,

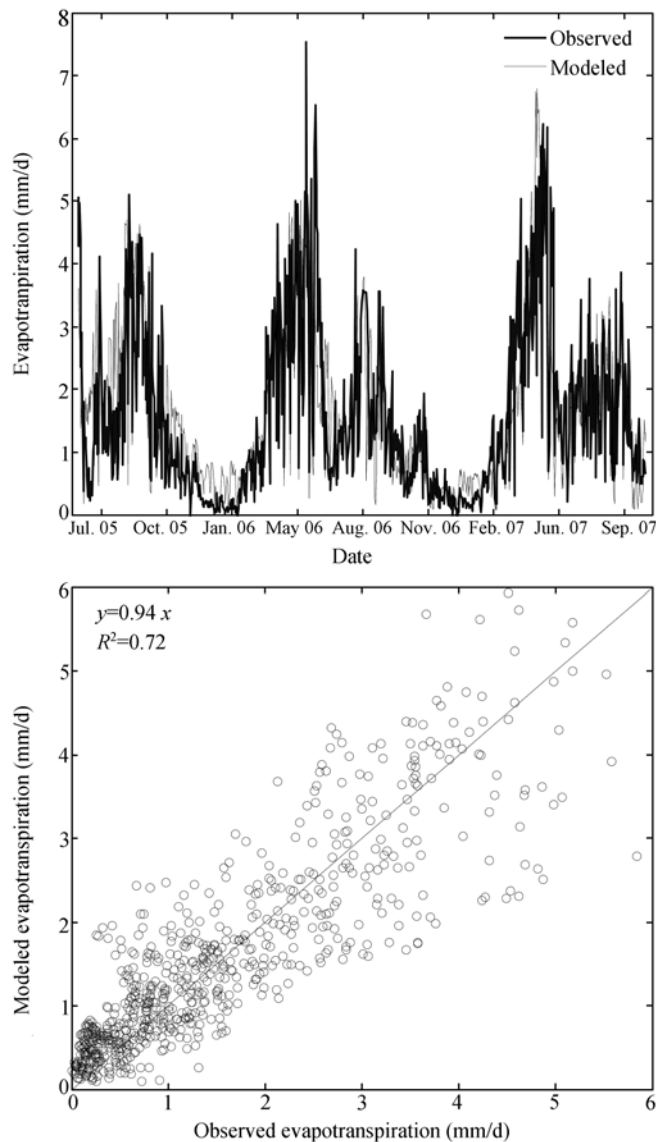


Figure 3 Measured and simulated evapotranspiration.

respectively) of the top soil layer during the period from June 1, 2005 to October 10, 2007. The total simulated evapotranspiration and CO_2 assimilation were in reasonable agreement with those measured, except for the CO_2 assimilation in the winter wheat seasons, due to the low accuracy of the optimized vegetation cover in winter (Table 2). The relative errors of ET and A_g were 3.8% and 4.5%, respectively. The model is capable of capturing the seasonal dynamics of both physiological and hydrological processes. This indicated that the model was applicable for both C_3 and C_4 plants and that the adaptation of annual crops to the environment can be achieved within a shorter period than with perennial trees. The simulated daily CO_2 assimilation and evapotranspiration were also in good agreement with the measured values. For CO_2 assimilation, the slope was 0.93 and the coefficient of determination R^2 was 0.73; for evapotranspiration, the slope was 0.94 and R^2 was 0.72. One reason for this disagreement was the observed energy imbalance (the slope of daily $H+\lambda E$ vs.

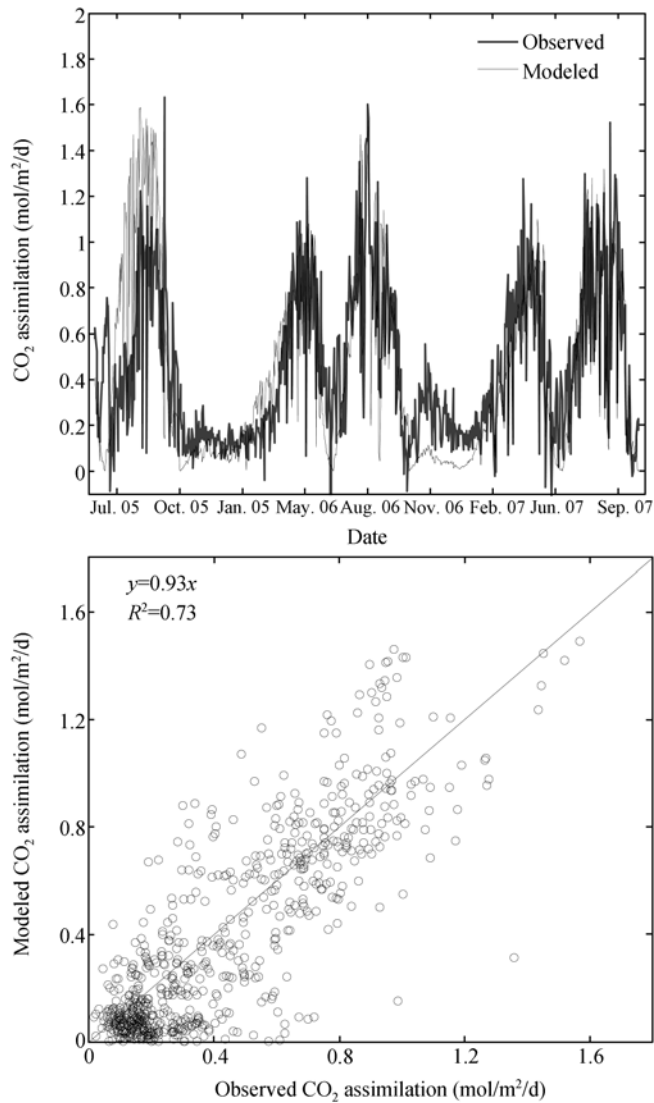


Figure 4 Measured and simulated CO₂ assimilation.

Table 2 Simulated and measured total evapotranspiration and CO₂ assimilation during the period

Item	Simulated	Measured	Relative error (%)
Total evapotranspiration (mm)	1434	1381	3.8
in the winter wheat seasons	745	744	0.1
in the summer maize seasons	689	637	8.2
Total CO ₂ assimilation (mol/m ²)	371	389	-4.5
in the winter wheat seasons	138	171	-19
in the summer maize seasons	233	218	7.0

R_n-G is 0.84), especially in the period with low vegetation cover, in which surface fluxes ($H + \lambda E$) were underestimated relative to estimates of available energy (R_n-G). Another reason was that the partitioning of measured canopy CO₂ exchange to CO₂ assimilation was not quite accurate. On the other hand, some of the increasing and declining parts were overestimated or underestimated, perhaps because the onset and offset of crop development were not captured exactly and especially

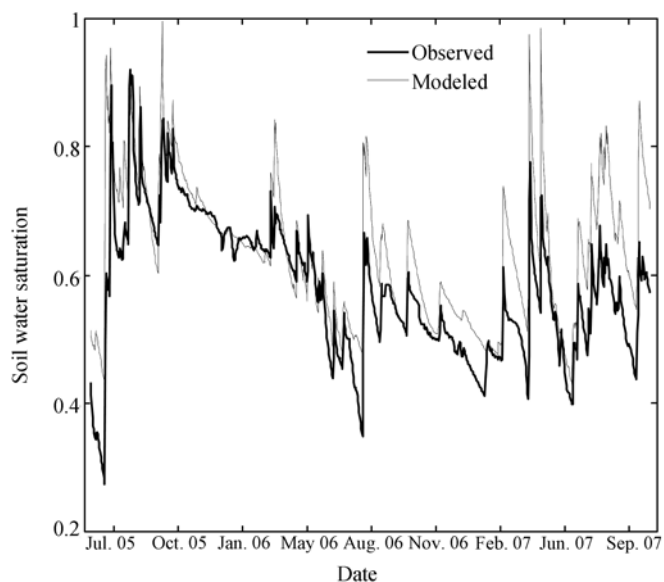


Figure 5 Measured and simulated soil water saturation of the top soil layer.

because the parameterization of carbon costs were oversimplified due to the lack of sufficient observations.

In the maize season in 2005, the simulated A_g was much over-predicted. One reason may be that the observed flux data during 2005-07-19 to 2005-08-19 were gap-filled, and another reason may be that the observed flux data were strongly disturbed by a highly dense rainfall that year, so that the data within all rainfall periods were also gap-filled. Soil moisture content was well simulated, which implies that both the root water uptake and canopy transpiration were modeled effectively. The disagreement in 2007 may be because the amount of irrigation was not estimated appropriately.

4.3 Evaluation of the optimality-based approach

The present model is not a complete self-organization model, but still needs empirical equations for constraining the optimization. It is unrealistic to consider all of the interactions between the environment and crops in a soil-vegetation-atmosphere model, due to the complexity of the system. Empirical models cannot capture the interaction between crops and the atmosphere; however, the process-based models require a complex parameterization scheme for crop behavior^[40,41]. A compromise is to combine the optimization with empirical equations. For example, leaf and root senescence cannot be modeled as a trade-off between the costs and the benefits of leaf CO_2 exchange, so we introduced the growing degree days to trigger the senescence of leaves and roots. The model was almost calibration free and therefore one would not expect to achieve a high R^2 value between observed and simulated daily CO_2 and transpiration fluxes; however, the vegetation hypothesis gave rise to a novel approach for modeling the interactions between vegetation and water balance, which needs no site-specific crop data (e.g. leaf area index) and few calibrated parameters based on local observations.

The Cowan and Farquhar constant λ theory employed in this model is useful for investigating the status of water use efficiency in crops. The λ value is a result of long-term adaptation of the crop to ambient soil water and climate. For one specific crop, λ is a one-to-one relationship with the

climate and water. Thus, scenarios with different combinations of irrigation, CO₂ concentration and climate condition can be used to investigate different crop behaviors in terms of λ value. It will be possible to determine optimum water use on the premise of the same CO₂ uptake achieved. In particular, it is capable of predicting the impact of climate change on crop water demand.

Owing to the simple and mechanistic parameterization scheme of crop transpiration, as a result of introducing the vegetation optimality, the optimality-based approach can be easily employed in a distributed hydrological model for developing a watershed ecohydrological model. Simulation of the regional soil-vegetation-atmosphere interactions by the watershed ecohydrological model is promising in terms of the improved management of regional water resources, especially in those regions where no direct vegetation information is available.

5 Conclusions

The agreement of simulations and measurements shows that the optimality-based model is applicable to both C₃ wheat and C₄ maize, and suggests that the optimality approach is useful for the agricultural land. Adaptation of an annual crop may be achieved in a short time period; however, the optimized crop properties did not agree well with reality. This was most likely due to the model assumptions and simplifications, as well as the simple parameterization of carbon costs of the Net Carbon Profit. Nevertheless, the vegetation optimality provides a novel approach to study crop behavior and its feedback to water balance, so that crop water consumption can be studied without prior knowledge of vegetation status. The optimality greatly simplifies the parameterization of vegetation and reduces the need for vegetation information (i.e. leaf area index), which potentially reduces the uncertainty of the model when the model is applied to the watershed where the vegetation data are not available. It will therefore be possible to study the optimum water use of crops under different climate and irrigation conditions, making this modeling system potentially useful for prediction of long-term responses of crops to climate change.

The authors would like to thank Michael Roderick from the Australian National University for helpful advice on the study and Jens Kattge from the Max-Planck Institute for Biogeochemistry for providing data about leaf dry mass and leaf life span for wheat and maize.

- 1 Cai X. Water stress, water transfer and social equity in Northern China-Implications for policy reforms. *J Environ Manage*, 2008, 87(1): 14–25[[doi](#)]
- 2 Yang D, Li C, Hu H, et al. Analysis of water resources variability in the Yellow River of China during the last half century using historical data. *Water Resour Res*, 2004, 40, W06502, [[doi](#)]
- 3 Allen R G, Pereira L S, Raes D, et al. *Crop Evapotranspiration Guidelines for Computing Crop Water Requirements*. Rome: Food and Agriculture Organization of the United Nations, 1998
- 4 Sellers P J, Randall D A, Collatz G J, et al. A revised land surface parameterization (SiB2) for atmospheric GCMS. Part I: model formulation. *J Climate*, 1996, 9(5): 676–705[[doi](#)]
- 5 Arora V K. Simulating energy and carbon fluxes over winter wheat using coupled land surface and terrestrial ecosystem models. *Agr Forest Meteorol*, 2003, 118(1): 21–47[[doi](#)]
- 6 Pauwels V R N, Verhoest N E C, De Lannoy G J M, et al. Optimization of a coupled hydrology-crop growth model through the assimilation of observed soil moisture and leaf area index values using an ensemble Kalman filter. *Water Resour Res*, 2007, 43, W04421, [[doi](#)]
- 7 Schymanski S J, Roderick M L, Sivapalan M, et al. A test of the optimality approach to modelling canopy properties and CO₂ uptake by natural vegetation. *Plant Cell Environ*, 2007,[[doi](#)]
- 8 Eagleson P S. Ecological optimality in water-limited natural soil-vegetation-systems 1. Theory and hypothesis. *Water Re-*

- sour Res, 1982, 18(2): 325–340[[doi](#)]
- 9 van der Tol C, Meesters A G C A, Dolman A J, et al. Optimum vegetation characteristics, assimilation, and transpiration during a dry season: 1. Model description. *Water Resour Res*, 2008, 44, W03421, [[doi](#)]
- 10 Schymanski S J, Sivapalan M, Roderick M L, et al. An optimality-based model of the dynamic feedbacks between natural vegetation and the water balance. *Water Resour Res*, 2008, [[doi](#)]
- 11 Farquhar G D, von Caemmerer S, Berry J A. A biochemical model of photosynthetic CO₂ assimilation in leaves of C₃ species. *Planta*, 1980, 149(1): 78–90[[doi](#)]
- 12 Medlyn B E, Dreyer E, Ellsworth D, et al. Temperature response of parameters of a biochemically based model of photosynthesis. II. A review of experimental data. *Plant Cell Environ*, 2002, 25(9): 1167–1179[[doi](#)]
- 13 Collatz G J, Ribas-Carbo M, Berry J A. Coupled photosynthesis-stomatal conductance model for leaves of C₄ plants. *Aust J Plant Physiol*, 1992, 19(4): 519–538
- 14 Givnish T J. Adaptation to sun and shade—a whole-plant perspective. *Aust J Plant Physiol*, 1988, 15(1-2): 63–92
- 15 Wohlfahrt G, Bahn M, Haubner E, et al. Inter-specific variation of the biochemical limitation to photosynthesis and related leaf traits of 30 species from mountain grassland ecosystems under different land use. *Plant Cell Environ*, 1999, 22(10): 1281–1296[[doi](#)]
- 16 Massad R, Tuzet A, Bethenod O. The effect of temperature on C₄-type leaf photosynthesis parameters. *Plant Cell Environ*, 2007, 30(10): 1191–1204[[doi](#)]
- 17 Todd G W. Photosynthesis and respiration of vegetative and reproductive parts of wheat and barley plants in response to increasing temperature. *Proc Okla Acad Sci*, 1982, 62(1): 57–62
- 18 Kim S, Gitz D C, Sicher R C, et al. Temperature dependence of growth, development, and photosynthesis in maize under elevated CO₂. *Environ Exp Bot*, 2007, 61(2): 224–236[[doi](#)]
- 19 Moss D N, Willmer C M, Crookston R K. CO₂ compensation concentration in maize (*Zea mays* L.). *Plant Physiol*, 1971, 47(7): 847–848[[doi](#)]
- 20 Schymanski S J, Sivapalan M, Roderick M L, et al. An optimality-based model of the coupled soil moisture and root dynamics. *Hydrol Earth Syst Sci*, 2008, 12(8): 913–932
- 21 Bryla D R, Bouma T J, Hartmond U, et al. Influence of temperature and soil drying on respiration of individual roots in citrus: integrating greenhouse observations into a predictive model for the field. *Plant Cell Environ*, 2001, 24(8): 781–790[[doi](#)]
- 22 Cowan I R, Farquhar G D. Stomatal function in relation to leaf metabolism and environment. In: Jennings D H, ed. *Integration of Activity in the Higher Plant*. Cambridge: Cambridge University Press, 1977. 471–505
- 23 Lizaso J I, Batchelor W D, Westgate M E. A leaf area model to simulate cultivar-specific expansion and senescence of maize leaves. *Field Crops Res*, 2003, 80(1): 1–17[[doi](#)]
- 24 Mao Z, Yu Z, Liu H. Experimental research on thermal requirement for winter wheat and its leaves (in Chinese). *J China Agr Univ*, 2002, 7(5): 14–19
- 25 Zhang Y, Yu Z, Driessen P M. Growing degree days requirements for plant and leaf development of summer maize (*Zea mays*) — An experimental and simulation study (in Chinese). *Chin J Appl Ecol*, 2001, 12(4): 561–565
- 26 Tojosoler C M, Sentelhas P C, Hoogenboom G. Thermal time for phenological development of four maize hybrids grown off-season in a subtropical environment. *J Agr Sci*, 2005, 143(2): 169–182[[doi](#)]
- 27 Carsel R F, Parrish R S. Developing joint probability distributions of soil water retention characteristics. *Water Resour Res*, 1988, 24(6): 755–769[[doi](#)]
- 28 Lim P O, Hyo J K, Hong G N. Leaf senescence. *Annu Rev Plant Biol*, 2007, 58(1): 115–136[[doi](#)]
- 29 McMaster G S, Wilhelm W W. Growing degree-days: one equation, two interpretations. *Agr Forest Meteorol*, 1997, 87(2): 291–300[[doi](#)]
- 30 Siddique K H M, Belford R K, Tennant D. Root: shoot ratios of old and modern, tall and semi-dwarf wheat in a Mediterranean environment. *Plant Soil*, 1990, 121(1): 89–98[[doi](#)]
- 31 Gavito M E, Curtis P S, Mikkelsen T N, et al. Interactive effects of soil temperature, atmospheric carbon dioxide and soil N on root development, biomass and nutrient uptake of winter wheat during vegetative growth. *J Exp Bot*, 2001, 52(362): 1913–1923[[doi](#)]
- 32 Ryu Y, Baldocchi D D, Ma S, et al. Interannual variability of evapotranspiration and energy exchange over an annual grassland in California. *J Geophys Res*, 2008, 113, D09101, [[doi](#)]
- 33 Foken T, Wichura B. Tools for quality assessment of surface-based flux measurements. *Agr Forest Meteorol*, 1996, 78(1): 83–105[[doi](#)]

- 34 Reichstein M, Falge E, Baldocchi D D, et al. On the separation of net ecosystem exchange into assimilation and ecosystem respiration: review and improved algorithm. *Glob Change Biol*, 2005, 11(10): 1424–1439[[doi](#)]
- 35 Fang C, Moncrieff J B. The dependence of soil CO₂ efflux on temperature. *Soil Biol Biochem*, 2001, 33(1): 155–165[[doi](#)]
- 36 Liu C, Zhang X, Zhang Y. Determination of daily evaporation and evapotranspiration of winter wheat and maize by large-scale weighing lysimeter and micro-lysimeter. *Agr Forest Meteorol*, 2002, 111(1): 109–120[[doi](#)]
- 37 Duan Q Y, Sorooshian S, Gupta V K. Optimal use of the SCE-UA global optimization method for calibrating watershed models. *J Hydrol*, 1994, 158(3-4): 265–284[[doi](#)]
- 38 Wullschleger S D. Biochemical limitations to carbon assimilation in C₃ plants—a retrospective analysis of the A/C_i curves from 109 species. *J Exp Bot*, 1993, 44(262): 907–920[[doi](#)]
- 39 Jackson R B, Mooney H A, Schulze E D. A global budget for fine root biomass, surface area, and nutrient contents. *Proc Natl Acad Sci*, 1997, 94: 7362–7366[[doi](#)]
- 40 Wang J, Yu Q, Lee X. Simulation of crop growth and energy and carbon dioxide fluxes at different time steps from hourly to daily. *Hydrol Proc*, 2007, 21: 2474–2492[[doi](#)]
- 41 Monteith J L. The quest for balance in crop modeling. *Agron J*, 1996, 88(5): 695–697